Optically detected electron paramagnetic resonance by microwave modulated magnetic circular dichroism

Birgit Börger, Stephen J. Bingham, Jörg Gutschank, Marc Oliver Schweika, and Dieter Suter
Fachbereich Physik, Universität Dortmund, 44221 Dortmund, Germany

Andrew J. Thomson
Centre for Metalloprotein Spectroscopy and Biology, School of Chemical Sciences, University of East Anglia, Norwich NR4 7TJ, United Kingdom

(Received 28 July 1999; accepted 16 August 1999)

Electron paramagnetic resonance (EPR) can be detected optically, with a laser beam propagating perpendicular to the static magnetic field. As in conventional EPR, excitation uses a resonant microwave field. The detection process can be interpreted as coherent Raman scattering or as a modulation of the laser beam by the circular dichroism of the sample oscillating at the microwave frequency. The latter model suggests that the signal should show the same dependence on the optical wavelength as the MCD signal. We check this for two different samples [cytochrome *c*-551, a metalloprotein, and ruby (Cr^{3+}:Al_2O_3)]. In both cases, the observed wavelength dependence is almost identical to that of the MCD signal. A quantitative estimate of the amplitude of the optically detected EPR signal from the MCD also shows good agreement with the experimental results. [S0021-9606(99)00842-9]

I. INTRODUCTION

Magnetic circular dichroism (MCD) spectroscopy measures the difference between the absorption of left and right circularly polarized light induced by a magnetic field along the direction of propagation of the light.[1,2] The major contribution to the MCD signal at cryogenic temperatures arises from a thermal population difference between the Zeeman components of the groundstate. The MCD signal is in the linear limit therefore proportional to the magnetization component along the static magnetic field.

The MCD signal can also be used to detect microwave resonances in the ground level. In this form of ODMR spectroscopy a microwave field partially saturates the spin transition and disturbs the equilibrium magnetization while the change of MCD is monitored at a fixed optical wavelength as a function of the magnetic field. This technique can be used to measure spin-lattice relaxation[3–5] or to distinguish paramagnetic centers with different optical absorption bands.[6–8] In addition, in samples such as frozen aqueous solutions of metalloproteins, where the molecules are randomly orientated, information about the relative orientations of magnetic and optical axes can be obtained.[6]

A different approach to optically detected electron paramagnetic resonance (ODEPR) uses coherent Raman scattering.[9,10] This technique detects the *transverse* component of the precessing magnetization in analogy to a conventional EPR experiment. Transitions of the electron spin are excited with a microwave field perpendicular to the static magnetic field. The transverse magnetization gives rise to coherent Raman scattering of a laser beam interacting with the paramagnetic center. The scattered Raman radiation can be detected by separating it from the incident laser radiation with a Fabry–Perot interferometer[11,12] or by optical heterodyne detection.[13]

As an alternative to the coherent Raman picture, this experiment can also be considered as a measurement of an oscillating circular dichroism induced by the precessing transverse magnetization of the electron spin.[14–16] A circularly polarized light beam is thus amplitude modulated at the microwave frequency. It is the purpose of this paper to discuss the implications of this model and to assess its validity by comparing experimental results from two prototypical systems; a frozen, aqueous solution of the metalloprotein cytochrome *c*-551, and a single crystal of ruby (Cr^{3+}:Al_2O_3). In particular, the MCD picture of ODEPR implies that the dependence of the signal on the optical wavelength should mirror the MCD spectrum, which often shows a characteristic wavelength dependence.

II. THEORY

We consider a paramagnetic material, which is placed in a large static magnetic field oriented along the *z*-direction. In thermal equilibrium, the sample contains a magnetization M_z along the magnetic field direction. As is well known from conventional magnetic resonance, a microwave field applied close to a paramagnetic resonance excites a transverse component of the magnetization. The component oscillating in phase with the driving microwave field is referred to as the dispersion component, while the absorption component appears in quadrature phase. If the phenomenological Bloch equations are applicable, the absorption component reaches a maximum at the resonance condition. In the absence of saturation, it becomes

$$M_{xy} = \omega_{\mathrm{Rabi}} T_2 M_z , \tag{1}$$

where ω_{Rabi} is the Rabi frequency, T_2 the phase memory time, and M_z the longitudinal magnetization. M_{xy} also equals the peak-to-peak value of the dispersion component.

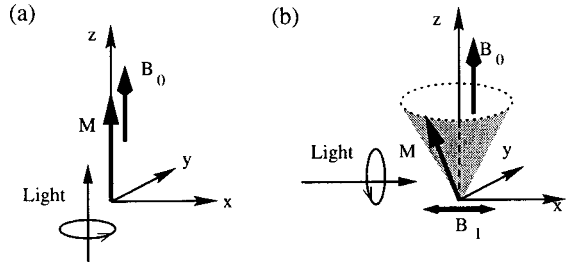

FIG. 1. (a) MCD geometry: the light beam parallel to the static magnetic field B_0 measures the longitudinal magnetization. (b) Geometry for transverse ODEPR. The microwave field B_1 causes precession of the magnetization around B_0. A circularly polarized laser beam probes the transverse component M_{xy}.

The conventional MCD signal ΔA_z, the differential absorption between left and right circularly polarized light, is proportional to the static magnetization along the field direction. The experimental configuration for a MCD experiment is illustrated in Fig. 1(a). Figure 1(b) shows the corresponding geometry for the transverse ODEPR experiment; the laser beam propagates perpendicular to the magnetic field. We assume here, that the transverse MCD along the laser beam direction is proportional to the transverse component M_{xy} of the magnetization and that the proportionality factor is the same as in the case of longitudinal MCD. For resonant microwave excitation, the transverse MCD is then

$$\Delta A_{xy} = \omega_{\mathrm{Rabi}} T_2 \Delta A_z . \tag{2}$$

A circularly polarized light beam passing through the sample is amplitude modulated at the microwave frequency ω_1 as

$$P = P_0 10^{-(A_0 + (\Delta A_{xy}/2)\sin \omega_1 t)}$$
$$\simeq P_{\mathrm{d.c.}} - P_0 10^{-A_0} \ln(10) \frac{\Delta A_{xy}}{2} \sin \omega_1 t, \tag{3}$$

where P_0 and P is the light power before and after the sample, respectively, A_0 the absorption of the unpolarized sample, and $P_{\mathrm{d.c.}}$ a d.c. offset. The amplitude of the modulated part represents the ODEPR signal. For small modulations (typically $\Delta A_{xy} \simeq 10^{-6}$ in our experiment), it is thus directly proportional to ΔA_{xy} and therefore to ΔA_z. The wavelength dependence of the ODEPR signal will therefore reflect that of the longitudinal MCD.

The concept of a microwave modulated MCD is valid as long as the linewidth of the optical transition is much broader than the microwave frequency.[15] This means that the concept of an optical transition probability is valid on a time scale much shorter than the Larmor period.

At this point, we wish to point out the limitations of this model. The assumption that the Bloch equations are valid implies that the EPR resonance line has a Lorentzian shape. This is usually not the case for systems with inhomogeneously broadened lines, especially for powderlike samples as investigated in our experiments. Accordingly, the present analysis is only semiquantitative. Furthermore, the calculation does not take any saturation of the EPR transition into account. While saturation may lead to a complete disappearance of the absorption, this effect is weaker for the dispersion or may not occur at all for an inhomogeneously broadened line.[17] The simplifications and estimates which have to be made to apply the presented theoretical approach to the real systems will also be described in the discussion of the experimental data.

III. EXPERIMENTAL APPARATUS AND SAMPLES

For the measurement of the coherent Raman detected EPR spectra the sample was placed in a rectangular cavity and excited by a weak microwave field with a frequency of $\simeq$13.6 GHz. A variable magnetic field (0–1 T) is provided by a superconducting split coil magnet. A laser beam parallel to the microwave field detects the precessing magnetization; the wavelength range accessible with our tuneable dye-laser (a Coherent 899 laser operating with Rhodamin 6G) is approximately 568–610 nm. The amplitude modulation of the light is detected with a high speed photodiode (bandwidth 21 GHz). Demodulation of this microwave signal in a quadrature mixer allows the simultaneous detection of absorption and dispersion components of the EPR signal. The polarizations of the light is modulated between right and left circularly polarized by a photoelastic modulator. A more detailed discussion of this instrument is published elsewhere.[13]

The broadband MCD spectrum of ruby was recorded using a commercial JASCO J-500 D spectrometer which employs a lamp as a light source. A high-resolution scan over a limited wavelength range was measured with a setup involving a dye-laser.

The single crystal of ruby (Cr^{3+}:Al_2O_3) investigated in our experiments has a nominal concentration of 2×10^{-3} Cr:Al. The light beam passed along the crystalline *c*-axis with a pathlength of 2 mm.

A buffered aqueous solution of low-spin ferric haem protein cytochrome *c*-551 from *Pseudomonas aeruginosa* was mixed with a glassing agent (ethanediol 1:1 vol.) to obtain good optical glass quality at low temperatures. The concentration was approximately 2.9 mM. The optical pathlength was 0.5 mm for the ODEPR experiment.

IV. EXPERIMENTAL RESULTS AND DISCUSSION

A. Cytochrome *c*-551

The protein cytochrome *c*-551 contains a low-spin ferric haem with spin $S=1/2$ ground level. Due to the large *g*-anisotropy [$g_z=3.2$, $g_y=2.05$, and $g_x\simeq1$ (Ref. 18)] the EPR spectrum of a frozen solution is strongly broadened. A dispersion type ODEPR spectrum measured at $\lambda=587.5$ nm is depicted in Fig. 2(a). The spectrum is presented in units of ΔA_{xy} which can be obtained from Eq. (3), using an accurate calibration of the instrument.[13] The line shape of the ODEPR signal differs from that of the conventional EPR spectrum because molecules for which the *g*-value *z*-axis (normal to the haem plane) is oriented parallel to the magnetic field do not contribute to the signal.[19] In the following discussion we approximate the EPR line shape by a Lorentzian. This allows us to introduce a ''resonant field'' B_r, as indicated in Fig. 2(a).

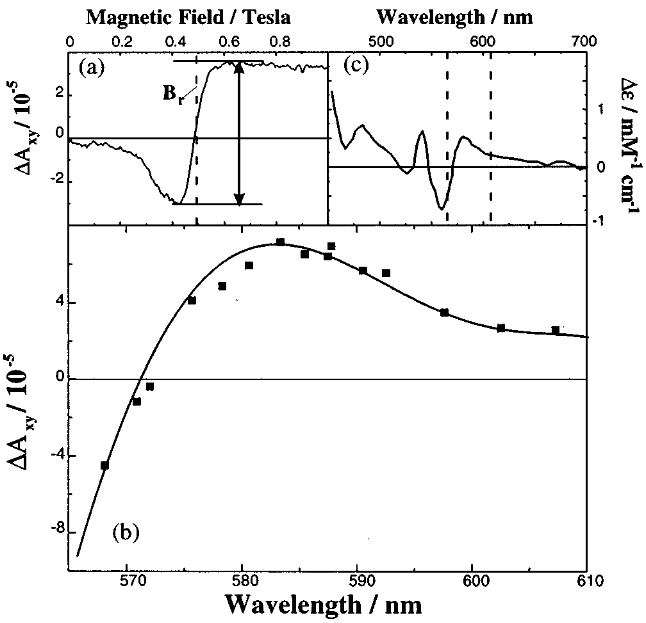

FIG. 2. (a) ODEPR spectrum of cytochrome *c*-551, $\lambda=587.5$ nm, $\vartheta=2.2$ K, $\omega_1/2\pi=13.66$ GHz. (b) Amplitude of ODEPR spectra as a function of wavelength (squares); scaled longitudinal MCD (solid line). (c) Longitudinal MCD of cytochrome *c*-551 at $B_0=4.9$ T and $\vartheta=4.2$ K (Ref. 20); the wavelength range of (b) is indicated by vertical lines.

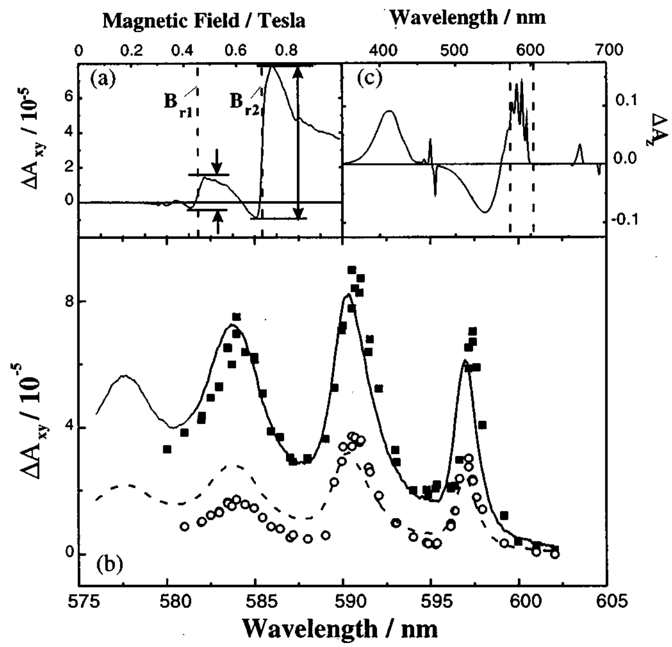

FIG. 3. (a) ODEPR spectrum of ruby, $\omega_1/2\pi=13.66$ GHz, $\vartheta=1.6$ K. (b) Amplitude of ODEPR resonances as a function of wavelength at B_{r1} (circles) and B_{r2} (squares); scaled MCD longitudinal (dashed and solid lines). (c) Longitudinal MCD of ruby recorded at $B_0=4.9$ T and temperature $\vartheta=1.6$ K. The scan has lower resolution than the MCD curve shown in (b); the wavelength range of (b) is indicated with vertical lines.

Although the absorption component of the EPR signal is strongly saturated at these experimental conditions, the dispersion signal is unaffected. Measurements at different temperatures show similar line shapes, while the amplitude is inversely proportional to the sample temperature. We may therefore use the peak-to-peak amplitudes as a measure of the transverse MCD ΔA_{xy}. Its dependence on the optical wavelength is indicated by square symbols in Fig. 2(b). The longitudinal MCD of cytochrome *c*-551 was first measured by Foote *et al.*[20] and is reproduced in Fig. 2(c). The magneto-optical spectrum shows broad vibronic transitions which are a feature common to all metalloproteins. The spectrum is given in units of the extinction coefficient $\Delta\epsilon$, which is proportional to the differential absorption via the equation $\Delta A=\Delta\epsilon cl$ (*c*, concentration; *l*, optical pathlength). We compare the wavelength dependence of the transverse MCD with that of the longitudinal MCD which is scaled by a factor of 1.1×10^{-4} and represented by the full line in Fig. 2(b). The comparison shows that the ODEPR spectra mirror the MCD wavelength characteristics, which is especially emphasized by the change of sign around 572 nm.

We now estimate the ratio between MCD and transverse ODEPR signal as discussed in the Theory. The width of the optical transition is large enough to satisfy the requirement that the linewidth of the optical excitation be much bigger than the microwave frequency. Since the experimental conditions were different for the measurements of MCD and transverse ODEPR, we first calculate the scaling factor between the parameters used for the MCD (magnetic field $B=4.9$ T, temperature $\vartheta=4.2$ K) and those for the ODEPR measurement (magnetic field $B'=B_r$, temperature $\vartheta'=2.2$ K). According to Ref. 1, the two values are related by

$$\Delta A_z(B,\vartheta)=\Delta A_z(B',\vartheta')\,\frac{\tanh(g\mu_B B/2k\vartheta)}{\tanh(g\mu_B B'/2k\vartheta')} \tag{4}$$

for a spin $S=1/2$ system, where g is the g-value of the paramagnetic species, μ_B is the Bohr magneton, and k is Boltzmann's constant.

Inserting ΔA_z in Eq. (2) yields the transverse MCD ΔA_{xy}. From the observed linewidth of the ODEPR spectrum we find $T_2\simeq2.7\times10^{-11}$ s; the Rabi-frequency was estimated as $\omega_{\mathrm{Rabi}}/2\pi=1.55$ MHz. The scaling factor thus becomes 5.5×10^{-5}, which agrees with the experimentally determined scaling factor within a factor of $\simeq2$, which is rather gratifying given the uncertainties in the determination of several experimental parameters (e.g., T_2, ω_{Rabi}.)

B. Ruby

Ruby contains Cr^{3+} ions in an axially symmetric environment. The $3d^3$ electrons of the chromium give rise to a spin $S=3/2$ electronic ground level, resulting in four Zeeman components.[21,22] At a microwave frequency of 13.66 GHz, six EPR transitions can in principle be observed. Of these, the low-field transitions are only weakly allowed in our experimental configuration where B_0 is perpendicular to the *c*-axis.

Figure 3(a) gives an example of an ODEPR spectrum ($\lambda=591$ nm, temperature 1.6 K). The absorption component of the signal is completely power saturated at such low temperatures. Also the dispersion shows saturation, resulting in a strong broadening of the EPR transitions. As temperature dependent studies showed, the spectra at temperatures higher than 70 K, where also an absorption type line shape is visible, show no distortion from saturation.[23] However, the studies presented in this paper have been performed at very low temperatures to obtain large signals whose wavelength dependence can easily be investigated.

For the following discussion we consider the two EPR transitions at high field, $B_{r1} \simeq 0.47$ T and $B_{r2} \simeq 0.7$ T [see Fig. 3(a)]. The peak-to-peak amplitude of the dispersion signal for these two transitions is plotted as a function of the optical wavelength in Fig. 3(b). The circles relate to the transition at B_{r1} and the squares to B_{r2}.

The MCD spectrum of ruby is shown in Fig. 3(c). The data were obtained at a temperature of 1.6 K in a magnetic field $B_0 = 4.9$ T aligned along the crystal *c*-axis. The optical transition is from the $^4A_2$ ground state to the ^4E excited state.[24,25] Single crystal studies showed all vibronic lines of this transition to be *xy*-polarized.[26] The wavelength range covered by the dye laser is indicated by the dashed vertical lines. In Fig. 3(b), the dashed and full curves represent the MCD, which has been scaled to simplify comparison with the ODEPR data. Comparison of the ODEPR signal amplitudes with the scaled MCD data shows that the dependence on the optical wavelength is qualitatively identical for the two data sets. Both data sets clearly exhibit the structure of the first three vibronic lines.

The simple quantitative estimate of the signal amplitude presented in Sec. II is not directly applicable to the spin $S = 3/2$ system of ruby. However, a straightforward extension to a four-level system yields again a value that is within an order of magnitude of the experimental result. Furthermore, the signal amplitudes show the same temperature dependence as the MCD signal.

V. CONCLUSION

Optical detection of electron paramagnetic resonance with a laser beam propagating perpendicular to the static magnetic field can be described as a coherent Raman process or, as we have discussed in this paper, as a transverse MCD induced by the precessing magnetization component. The modulation occurs therefore at the microwave frequency and can be measured by phase-sensitive detection. The MCD model of transverse ODEPR implies that the signal should show the same dependence on the optical wavelength as the MCD signal, with a scaling factor that can be estimated from the spectral parameters of the system. These consequences were verified on two prototypical samples, an oriented single crystal and a frozen glass in which molecules are randomly oriented. Deviations from this behavior may be expected when additional effects become important, such as spectral holeburning.

The results are important for planning future ODEPR measurements since the size of the ODEPR signal can be estimated and experimental parameters, particularly the optical wavelength, optimized with the described approach. Especially for deconvoluting overlapping EPR spectra from centers with different optical properties the choice of the optical wavelength is essential.

It is very attractive to apply the presented model to the detailed analysis of ODEPR spectra from metalloproteins in frozen aqueous solution. As already described for cytochrome *c*-551, the ODEPR spectra show additional features due to orientational selectivity via the electric dipole transitions of the molecule. A description of the experiment using the well-known theories of EPR and magneto-optical spectroscopy enables a satisfactory analysis of the experimental spectra and can thus give additional information about the correlations between magnetic and optical properties of the protein's active site.[27]

ACKNOWLEDGMENTS

We thank Dr. Jaqui A. Farrar for her experimental assistance during the preparation of the protein sample. We gratefully acknowledge the support by the UK Royal Society and the DFG through the Graduiertenkolleg Festkörperspektroskopie.

[1] A. J. Thomson, M. R. Cheesman, and S. J. George, Methods Enzymol. **226**, 199 (1993).
[2] J. C. Sutherland, Methods Enzymol. **246**, 110 (1995).
[3] S. Geschwind, *Electron Paramagnetic Resonance* (Plenum, New York, 1972).
[4] K. J. Standley and R. A. Vaughan, *Electron Spin Relaxation Phenomena in Solids* (Plenum, New York, 1969).
[5] J. M. Daniels and K. E. Rieckhoff, Can. J. Phys. **38**, 604 (1960).
[6] C. P. Barrett, J. Peterson, C. Greenwood, and A. J. Thomson, J. Am. Chem. Soc. **108**, 3170 (1986).
[7] F. J. Ahlers, F. Lohse, J. M. Spaeth, and L. F. Mollenauer, Phys. Rev. B **28**, 1249 (1983).
[8] C. A. Moore and R. A. Satten, Phys. Rev. B **7**, 1753 (1972).
[9] T. Blasberg and D. Suter, Phys. Rev. B **51**, 12 439 (1994).
[10] N. C. Wong, E. S. Kintzer, J. Mlynek, R. G. DeVoe, and R. G. Brewer, Phys. Rev. B **28**, 4993 (1983).
[11] A. S. Borovik-Romanov and N. M. Kreines, Phys. Rep. **81**, 351 (1982).
[12] R. Romestain, S. Geschwind, G. E. Devlin, and P. A. Wolff, Phys. Rev. Lett. **33**, 10 (1974).
[13] S. J. Bingham, B. Börger, D. Suter, and A. J. Thomson, Rev. Sci. Instrum. **69**, 3403 (1998).
[14] H. G. Dehmelt, Phys. Rev. **105**, 1924 (1957).
[15] N. Bloembergen, P. S. Pershan, and L. R. Wilcox, Phys. Rev. **120**, 2014 (1960).
[16] L. L. Chase, Phys. Rev. Lett. **21**, 888 (1968).
[17] A. M. Portis, Phys. Rev. **91**, 1071 (1953).
[18] A. Dwivedi, W. A. Toscano, Jr., and P. Debrunner, Biochim. Biophys. Acta **576**, 502 (1979).
[19] B. Börger, Diploma thesis, University of Dortmund (unpublished), 1998.
[20] N. Foote, J. Peterson, P. M. A. Gadsby, C. Greenwood, and A. J. Thomson, Biochem. J. **223**, 369 (1984).
[21] A. Abragam and B. Bleaney, *Electron Paramagnetic Resonance of Transition Ions* (Oxford University Press, Oxford, 1970).
[22] M. M. Zaripov and I. I. Shamonin, Sov. Phys. JETP **3**, 171 (1956).
[23] S. J. Bingham, D. Suter, A. Schweiger, and A. J. Thomson, Chem. Phys. Lett. **266**, 543 (1997).
[24] S. Sugano, Y. Tanabe, and H. Kamimura, *Multiplets of Transition Metal Ions in Crystals* (Academic, London, 1970), Chap. 5.
[25] B. Henderson and G. F. Imbusch, *Optical Spectroscopy of Inorganic Solids* (Oxford University Press, Oxford, 1989), Chap. 9.
[26] R. A. Ford and O. F. Hill, Spectrochim. Acta **16**, 493 (1960).
[27] S. J. Bingham, B. Börger, J. Gutschank, D. Suter, and A. J. Thomson, JBIC (to be published).